Molecules of senescent glial cells differentiate Alzheimer's disease from ageing

Linbin Dai # 1 2 3, Feng Gao # 1 2, Qiong Wang 1 2, Xinyi Lv 1 2, Zhaozhao Cheng 1 2, Yan Wu 1 2, Xianliang Chai 1 2, Henrik Zetterberg 4 5 6 7 8, Kaj Blennow 4 5, Allan I Levey 9, Jiong Shi 1 2 10, Yong Shen 11 2 3 12 13; CANDI Consortium

1Department of Neurology, The First Affiliated Hospital of USTC, Division of Life Sciences and Medicine, University of Science and Technology of China, Hefei, People's Republic of China.

2Institute on Aging and Brain Disorders, The First Affiliated Hospital of USTC, Division of Life Sciences and Medicine, University of Science and Technology of China, Hefei, People's Republic of China.

3Neurodegenerative Disorder Research Center, School of Life Sciences, Division of Life Sciences and Medicine, Hefei National Laboratory for Physical Sciences at the Microscale, University of Science and Technology of China, Hefei, People's Republic of China.

4Department of Psychiatry and Neurochemistry, Institute of Neuroscience and Physiology, the Sahlgrenska Academy at the University of Gothenburg, Mölndal, Sweden.

5Clinical Neurochemistry Laboratory, Sahlgrenska University Hospital, Mölndal, Sweden.

6Department of Neurodegenerative Disease,UCL Institute of Neurology, Queen Square, London, UK.

7UK Dementia Research Institute at UCL, London, UK.

8Hong Kong Center for Neurodegenerative Diseases, Hong Kong, People's Republic of China.

9Department of Neurology, Goizueta Alzheimer's Disease Research Center, Emory University, Atlanta, Georgia, USA.

10China National Clinical Research Center for Neurological Diseases, Beijing Tiantan Hospital, Capital Medical University, Beijing, People's Republic of China.

11Department of Neurology, The First Affiliated Hospital of USTC, Division of Life Sciences and Medicine, University of Science and Technology of China, Hefei, People's Republic of China yongshen@ustc.edu.cn.

12Hefei National Laboratory for Physical Sciences at the Microscale, University of Science and Technology, Hefei, Anhui, China.

13Centre for Excellence in Brain Science and Intelligence Technology, Chinese Academy of Sciences, Shanghai, China.

#Contributed equally.

PMID: 37012067 DOI: 10.1136/jnnp-2022-330743

Abstract

Background: Ageing is a major risk factor for Alzheimer's disease (AD), which is accompanied by cellular senescence and thousands of transcriptional changes in the brain.

Objectives: To identify the biomarkers in the cerebrospinal fluid (CSF) that could help

differentiate healthy ageing from neurodegenerative processes.

Methods: Cellular senescence and ageing-related biomarkers were assessed in primary astrocytes and postmortem brains by immunoblotting and immunohistochemistry. The biomarkers were measured in CSF samples from the China Ageing and Neurodegenerative Disorder Initiative cohort using Elisa and the multiplex Luminex platform.

Results: The cyclin-dependent kinase inhibitors p16/p21-positive senescent cells in human postmortem brains were predominantly astrocytes and oligodendrocyte lineage cells, which accumulated in AD brains. CCL2, YKL-40, HGF, MIF, S100B, TSP2, LCN2 and serpinA3 are biomarkers closely related to human glial senescence. Moreover, we discovered that most of these molecules, which were upregulated in senescent glial cells, were significantly elevated in the AD brain. Notably, CSF YKL-40 (β=0.5412, $p<0.0001$) levels were markedly elevated with age in healthy older individuals, whereas HGF (β=0.2732, p=0.0001), MIF (β=0.33714, p=0.0017) and TSP2 (β=0.1996, p=0.0297) levels were more susceptible to age in older individuals with AD pathology. We revealed that YKL-40, TSP2 and serpinA3 were useful biomarkers for discriminating patients with AD from CN individuals and non-AD patients.

Discussion: Our findings demonstrated the different patterns of CSF biomarkers related to senescent glial cells between normal ageing and AD, implicating these biomarkers could identify the road node in healthy path off to neurodegeneration and improve the accuracy of clinical AD diagnosis, which would help promote healthy ageing.

Abbreviations

Aβ = amyloid-β; *APOE* = apolipoprotein E; CCL2 = C-C motif chemokine ligand 2; CDR = Clinical Dementia Rating; CN = normal cognition; HGF = hepatocyte growth

factor; IHC = immunohistochemistry; LCN2 = lipocalin-2; LOWESS = locally-weighted scatterplot smoothing; LR = logistic regression; MIF = macrophage migration inhibitory factor; MMSE = Mini-Mental State Examination; ROC = receiver operating characteristic; S100B = S100 calcium-binding protein B; SA-β-gal = senescence-associated beta-galactosidase; serpinA3 = serine proteinase inhibitor A3; TSP2 = thrombospondin 2; VEGF = vascular endothelial growth factor; YKL-40 = chitinase 3-like 1

Introduction

Population aging and age-related disorders are major social problems facing world, and healthy aging is a common need of human society. One of the prominent problems brought about by the aging of the population is the high incidence of aging-related diseases, which leads to heavy socio-economic and medical burdens. Therefore, improving the level of diagnosis, treatment and prevention of aging-related diseases and achieving healthy aging is a major social need that urgently needs to be addressed. Alzheimer's disease (AD) is an age-related neurodegenerative disorder in which memory decline and cognitive degeneration progressively worsen with age (*1*). Cellular senescence, which is defined as a state of cell growth arrest (*2*), is considered a hallmark of aging and is a powerful driver of aging-related diseases, including neurodegenerative disorders (*3, 4*). Indeed, the abnormal accumulation of senescence markers such as $p16^{INK4a}$ and CDK4 has been observed in the brains of AD patients (*5*-*8*). In addition, the activity of senescence-associated beta-galactosidase (SA-β-gal) is also elevated in the plasma of AD patients (*9*). Therefore, cellular senescence may be involved in AD pathogenesis.

Glial cells, consisting of astrocytes, microglia, and oligodendrocyte lineage cells, exhibit senescence phenotypes in the brain (*8, 10, 11*). Glial cells are a major component of the central nervous system (CNS) and are pivotal in the maintenance of neuronal homeostasis, blood-brain barrier integrity, and the regulation of neuroinflammation (*12, 13*). During aging, glial cells, but not neurons, show a more dominant alteration of

aging-related gene expression in the human brain (*14*). Notably, it has been suggested that AD-characterized pathologies, including amyloid-β (Aβ) deposition and tau aggregation, exacerbate glial-cell senescence (*8, 11*). Senescent glial cells not only undergo loss of essential function, but also upregulate a variety of pro-inflammatory molecules including cytokines, chemokines, and proteases, which contribute to CNS pathology (*15-17*). Accordingly, clearance of senescent glial cells markedly prevents brain pathology and reduces cognitive impairment in an AD mouse model (*10, 11*). These findings suggest that senescent glial cells may contribute to the pathogenesis of AD during aging and highlight the potential value of senescent glial cells as a therapeutic target for AD intervention. However, there was no known feasible method of evaluating the senescence status of glial cells in the living human brain.

In this study, we first evaluated postmortem the senescent brain cells in AD patients and age-matched individuals. We then investigated several factors that are reported to be upregulated in the CNS during aging in a clinical cohort consisting of individuals who were cognitively normal (CN), or had mild cognitive impairment (MCI), AD dementia, or non-Alzheimer's dementia (non-AD). These factors include the molecules chemokine (CCL2) (*18*); hepatocyte growth factor (HGF) (*19*); inflammatory factors chitinase 3-like 1 (YKL-40) (*20, 21*), macrophage migration inhibitory factor (MIF) (*22*), lipocalin-2 (LCN2) (*15, 23*), calcium-binding proteins (S100B) (*24*), thrombospondin 2 (TSP2) (*16, 25*), and the protease inhibitor serine proteinase inhibitor A3 (serpinA3) (*15, 16, 26*). We identified that oligodendrocyte lineage cells and astrocytes were the major senescent cells in the human brain. Importantly, we observed that most of these related factors were highly upregulated in p16 positively senescent cells. Among these molecules, we not only identified potential cerebrospinal fluid (CSF) biomarkers (YKL-40, MIF) that may reflect glial cell aging but also revealed some factors (HGF, MIF, TSP2) that may reflect AD-related pathology-driven abnormal aging. These AD pathology-associated biomarkers not only improve the clinical diagnostic accuracy for AD but may also help evaluate the efficacy of targeted-senescent glial cell therapies for AD in the future.

Materials and methods

Participants

Participants were recruited from the First Affiliated Hospital of University of Science and Technology of China (USTC). This study included a total of 195 patients between the ages of 50 and 75, all of whom underwent lumbar punctures. Extracted CSF was divided into 200 µl aliquots and stored at -80 °C until measurements were taken. Participants who carried heterozygous or homozygous ε4 alleles were defined as *APOE*-ε4 carriers. Mini-Mental State Examination (MMSE) and Clinical Dementia Rating (CDR) scores were used to assess cognitive status. The diagnosis of mild cognitive impairment (MCI) and AD was based on the NIA-AA criteria of A-T-N (2011) (*27, 28*). Non-AD patients included those with cognitive disorders other than AD, such as Lewy body disease, frontotemporal dementia, vascular dementia, and Parkinson's disease dementia. This research study was approved by the ethics committee of the First Affiliated Hospital of University of Science and Technology China (2019KY-26). All patients provided written informed consent for this study. Brain tissues for western blotting and immunohistochemistry were from the Brain Bank and Neurodegenerative Disorder Research Center of USTC.

CSF Measurements

CSF Aβ40, Aβ42, P-tau181, and total tau were measured using the INNOTEST enzyme-linked immunosorbent assays (Fujirebio). SerpinA3 was measured using a commercially available ELISA kit (Sino Biological, SEK10307). All other analytes were measured using the multiplex Luminex platform (Luminex Corp, Luminex 200) and a R&D LXSAHA kit. All measurements were performed according to the manufacturer's instructions at the Neurodegenerative Disorder Research Center, University of Science and Technology of China, Hefei, China.

Aβ and tau status classifications

Aβ status and tau status were defined by the CSF Aβ42/ Aβ40 ratio and CSF P-tau, respectively (*29*). The cutoff values in our cohort were computed by the receiver operating characteristic (ROC) curves using SPSS 26.0 (SPSS. Inc, IBM) and determined using the highest Youden index method. ROC curves were used to discriminate AD patients from the others including cognitively normal (CN), MCI, and non-AD patients. The resulting cutoff of the Aβ42/40 ratio was 0.0617 (A+: Aβ42/40<0.0617), and 64.68 pg/ml for P-tau (T+: P-tau>64.68).

APOE genotyping

Genomic DNA was purified from 200 μl whole blood using EasyPure Blood Genomic DNA kit (TransGen Biotech, EE121-11) according to the manufacturer's instructions. Genomic DNA was then carried out to amplify a 268-bp DNA fragment with the following primers: F-5'GGCACGGCTGTCCAAGGA and R-5'CTCGCGGATGGCGCTGAG. Next, HhaI (NEB, R0139S) was added to the mixture of PCR products for restriction enzyme digestion. Finally, the reaction mixture was loaded onto 12% polyacrylamide non-denaturing gel and electrophoresed for 3 hours under constant current-voltage (80 V). *APOE* genotype was determined according to the size of HhaI fragments visualized by UV transillumination following the unique digestion pattern: *APOE2/2* (91bp and 83bp); *APOE2/3* (91bp, 83bp,48bp, and 35bp); *APOE2/4*(91bp, 83bp,72bp, 48bp, and 35bp); *APOE3/3* (91bp, 48bp, and 35bp); *APOE3/4* (91bp, 72bp, 48bp, and 35bp), and *APOE4/4* (72bp, 48bp, and 35bp).

Western blotting

Human brain tissue (temporal cortex) was homogenized in RIPA buffer with Protease inhibitor cocktail (Roche) and PMSF (Sigma) on ice and then mixed with 2xSDS loading buffer. Proteins were loaded onto SDS-PAGE gels and then transferred into PVDF membranes followed by blocking the membranes and incubating with primary antibodies overnight at 4 °C. Membranes were incubated with peroxidase-conjugated secondary antibodies and SuperSignal Chemiluminescent Substrates (Thermo

Scientific), then detected by chemiluminescence autoradiography. The membranes were probed with following primary antibodies: anti-CCL2 (Proteintech, 25542-1-AP), anti-YKL-40 (Proteintech, 12036-1-AP), anti-HGF (ABclonal, A1193), anti-MIF (Abcam, ab65869), anti-S100B (Z031101-2, Dako), anti-TSP2 (Abcam, ab112543), anti-LCN2 (Abcam, ab63929), anti-serpinA3 (ABclonal, A1021), and GAPDH (Proteintech, 10494-1-AP).

Immunohistochemistry

Paraformaldehyde-fixed paraffin-embedded brain tissues were sectioned at a thickness of 6 μm. For immunohistochemical (IHC) staining, heat-induced epitope retrieval of sections was performed using a microwave oven with citric acid buffer and then 0.3% H_2O_2 in methanol for 20 min at room temperature. Next, sections were treated with 0.3% Triton X-100 in PBS for 30 min and then incubated with blocking buffer for 20 min at 37 °C, and thereafter with anti-p16 (Santa, sc-1661) diluted in antibody buffer overnight at 4 °C. After several washings, sections were incubated with secondary antibodies for 30 min at 37 °C and then incubated with VECTASTAIN Elite HRP Kit (Vectorlabs, PK-6100) and DAB Substrate Kit (Vectorlabs, SK-4100). For immunofluorescence co-staining, sections were pretreated as above and incubated with appropriate primary antibodies overnight at 4 °C. After washing, sections were incubated with fluorescent-labeled secondary antibody for 2 hours at room temperature. Section images were acquired using TissueFAXS PLUS (TissueGnostics) or confocal microscopy (Zeiss).

Statistical analysis

We excluded the extreme values of each potential CSF biomarker, which were those beyond three times the interquartile range above the third quartile (Q3) or those below the first quartile (Q1). Before comparisons, all CSF biomarker values were tested for normality using the Kolmogorov-Smirnov test. Values for HGF, TSP2, and the Aβ42/Aβ40 and P-tau/T-tau ratios, all had a normal distribution, whereas the other CSF biomarkers values did not follow a normal distribution and were thus log10-

transformed.

Categorical variables were tested using Pearson's Chi-square tests. MMSE and CDR values were compared using one-way analysis of covariance (ANCOVA) adjusted by age, sex, and education. CSF biomarkers were assessed by ANCOVA with adjustment for age and sex as covariates. These comparisons were followed by Bonferroni corrected post-hoc comparisons. Correlations between age and CSF biomarkers were tested using partial correlations adjusted by age, sex, and apolipoprotein E (*APOE*)-ε4 status.

The association of each CSF biomarker with age and AD pathology was evaluated with a LOWESS model and with a linear regression model with the adjustment for age, sex, and *APOE*-ε4 status. We performed logistic regression (LR) and computed the ROC to evaluate the discriminative accuracy of CSF biomarkers for discriminating different disease groups. LR analyses were performed using the variables age, gender, *APOE* states (0 for no *APOE*-ε4 carriers, 1 for *APOE*-ε4 carriers), T-tau, P-tau, Aβ40, Aβ42, Aβ42/Aβ40, P-tau/T-tau, and all measured potential biomarkers, with backward elimination.

Results

Senescent glial cells accumulate in the AD brain

To investigate senescent-cell status in the human AD brain, we performed immunohistochemistry for the marker p16 on the temporal cortex of AD patients and age-matched controls (details of these human tissues are listed in **Table 1**). A significant increase of p16-positive cells was observed in the AD brain (**Fig. 1A-B**). Importantly, p16 expression was elevated predominantly in Olig2- or glial fibrillary acidic protein (GFAP)-positive glial cells (**Supplementary Fig. 1A**), suggesting that oligodendrocyte lineage cells and astrocytes were the primary senescent cells in the AD brain. Of note, immunohistochemical analysis also revealed that these senescent cells expressed several aging-related molecules, including YKL-40, HGF, MIF, S100B, TSP2, LCN2,

and SerpinA3 (**Supplementary Fig. 1B**). Consistent with the observation that senescent cells accumulate in the AD brain, some of these molecules (i.e., YKL-40, HGF, MIF, and SerpinA3) were significantly higher in the AD brain (**Fig. 1C-D**). Thus, cellular senescence was exacerbated in the AD brain, which leads to an accumulation of aging-related molecules.

Assessment of aging-related molecules in the CSF

To investigate the relationship between the expression of aging-related molecules in CSF and AD pathology, we recruited 195 individuals including 58 (29.7%) individuals assessed to be cognitively normal (CN), 37 (19.0%) diagnosed with mild cognitive impairment (MCI), 78 (40.0%) clinically diagnosed with Alzheimer's disease (AD), and 22 (11.3%) defined as having non-Alzheimer's dementia (non-AD). There were no significant differences in gender or education between different groups, and the baseline characteristics are described in **Table 2**.

We summarized expression patterns of these molecules in four clinical diagnoses (CN, MCI, AD, and non-AD) (**Table 3**). Levels of CCL2, S100B, and LCN2 were similar amongst groups. Concentrations of YKL-40 and MIF were both the lowest in the CN group and were significantly different from those in the MCI and AD groups. In addition to YKL-40 levels, levels of SerpinA3 in the non-AD group were also higher than that in the CN group. There were higher HGF and TSP2 levels in the MCI and AD groups than in the non-AD group, and higher SerpinA3 levels in non-AD group than in either the MCI or AD groups. To study the association of each molecule with Aβ and tau pathology, a linear regression model was computed adjusting for age, gender, and *APOE* status (**Table 4**). We observed that CCL2 and S100B were only affected by Aβ pathology, whereas YKL-40, HGF, MIF, TSP2, LCN2, and SerpinA3 were affected by both Aβ and tau pathology.

To further accurately examine the effects due to dysregulation of these molecules on the development of Aβ and tau pathology, we performed locally weighted scatterplot smoothing (LOWESS) models (**Supplementary Fig. 2**). Interestingly, HGF, MIF and

SerpinA3 were dysregulated in the early stages of Aβ pathology (i.e., Aβ42/ Aβ40>0.04) and further dysregulated in the later stages. In contrast, HGF, MIF, S100B, and TSP2 were strongly dysregulated in the early stage of tau pathology but tended to stabilize in the late stage. This suggests that certain CSF senescent glial cell biomarkers are associated with specific stages of Aβ pathology and tau pathology.

CSF biomarker values stratified by AD pathology status and CDR score

To investigate the expression of these molecules at different stages of AD pathology, we classified participants into two groups based on Aβ status or tau status. Next, we compared the levels of these molecules in patients with or without AD pathology. There were considerable differences in all molecules tested, except CCL2 and S100, between levels found in Aβ-positive individuals (A+) and those found in Aβ-negative individuals (A−) (**Supplementary Fig. 3A-H**). In particular, YKL-40 (P=0.0004), HGF (P=0.0017), MIF (P<0.0001), and TSP2 (P=0.0051) were significantly higher in the A+ group than in the A− group. In contrast, in the A− group, there were significantly higher levels of LCN2 (P=0.0001) and serpinA3 (P<0.0001). Interestingly, similar patterns of molecule levels were also observed between the two tau states (**Supplementary Fig. 3I-P**).

We then evaluated differences in molecule levels in individuals with different levels of clinical dementia rating (CDR) scores and defined two groups: CDR=0 and CDR>0. (**Fig. 2**; **Supplementary Fig. 4)**. We found no differences in CCL2 (P=0.6677), HGF (P=0.8072), S100B (P=0.2487), TSP2 (P=0.1098), LCN2 (P=0.0855), or serpinA3 (P=0.7024) between CDR=0 and CDR>0 groups, whereas in individuals with CDR>0, YKL-40 (P<0.0001) and MIF (P<0.0001) were significantly higher than those with CDR=0 (**Fig. 2**). Within the CDR>0 group YKL-40, HGF, and TSP2 were elevated, whereas LCN2 and SerpinA3 were depressed in Aβ-positive individuals compared to Aβ-negative individuals. Interestingly, S100B levels were elevated in Aβ-positive individuals within the CDR=0 group (P=0.0404). Meanwhile, HGF and TSP2 were

elevated in tau-positive individuals within the CDR>0 group (**Supplementary Fig. 4D and 4F**). However, only the SerpinA3 biomarker was depressed in the tau-positive group within the CDR>0 group (**Supplementary Fig. 4H**). Importantly, MIF levels were robustly elevated in Aβ-positive or tau-positive individuals and were independent of cognitive performance (**Fig. 2D**; **Supplementary Fig. 4D**).

Trajectories of CSF biomarkers with age

We analyzed differences in these CSF biomarkers with age, with or without AD pathology. There was an association between biomarker levels in the majority of the molecules tested with age (except S100B, LCN2, and serpinA3) (**Table 5**). There was a significant association between CCL2 and age in the A− group but not the A+ group, whereas there was a significant association of HGF and TSP2 with age only in the A+ group **(Fig. 3)**. In contrast, YKL-40 and MIF were positively correlated with age regardless of Aβ status (**Fig. 3**). Likewise, HGF and MIF were also correlated with age regardless of tau status (**Supplementary Fig. 5**). Importantly, expression of HGF, MIF, and TSP2 was exacerbated with age under AD-related Aβ or tau pathology, whereas CCL2 and YKL-40 were more susceptible to age in the absence of AD pathology (as shown by the β slopes).

CSF biomarkers in differential diagnosis of AD

To investigate whether these molecules could improve discriminatory capacity for clinical diagnosis, we performed logistic regression (LR) analysis using the variables of *APOE* status and all CSF biomarkers, with backward elimination. We found that only YKL-40, in addition to Aβ and tau, improved diagnostic accuracy and facilitated discrimination between individuals with MCI, AD, and non-AD from the CN group (**Fig. 4A-C**). Remarkably, serpinA3 (P=0.047) and TSP2 (P=0.030) were significant contributors in the LR analysis that helped distinguish AD from non-AD. We used the predicted value calculated by the LR model as an independent variable to compute its discriminative accuracy for distinguishing AD patients from non-AD patients. We

observed that the LR model (including T-tau, Aβ42, TSP2, serpinA3, and *APOE* state) was better able (AUC=0.963) than Aβ42/ Aβ40 (AUC=0.877) and P-tau (AUC=0.867) to discriminate between individuals with AD from those with non-AD **(Fig. 4D**). These results suggest that YKL-40 might be helpful not only in the diagnosis of AD but also in differentiation between individuals of CN and MCI as well as non-AD. More importantly, serpinA3 and TSP2 are potential clinical diagnostic biomarkers that may improve upon current discriminative accuracy of AD patients from non-AD patients.

Discussion

In this cross-sectional study, we aimed to identify CSF biomarkers of AD pathology-driven CNS senescence in a well-characterized cohort of individuals with or without AD pathology. The main findings of the present study are as follows: (1) glial cells (i.e., oligodendrocyte lineage cells and astrocytes) were the major senescent cells in the AD brain; (2) CSF levels of YKL-40, HGF, MIF, S100B, TSP2, LCN2, and serpinA3 were associated with AD pathology; (3) levels of CSF molecules, including YKL40, and MIF, were upregulated in normal aging, whereas HGF, MIF, and TSP2 were further dysregulated and thus greatly susceptible to AD pathology in aging, and (4) CSF levels of YKL-40 help distinguish patients with MCI, AD, or non-AD from CN, while serpinA3 and TSP2 may improve discriminative ability between AD and non-AD patients.

Transcriptional and functional changes in glial cells have been well studied in both physiological aging and AD models in both humans and mouse models (*14, 15, 30*). These studies reveal that normal physiological aging induces A1-like astrocyte reactivity and that cumulative exposure to AD pathological stimuli also renders glial cells senescent and more reactive. Consistently, all presently studied aging-related molecules (except CCL2) were predominantly expressed in senescent glial cells. Importantly, there were higher levels of almost all molecules tested as age increased within the present cohort, implying that these biomarker molecules may be a useful reflection of CNS aging.

Meanwhile, fairly high correlations between these molecules and CSF AD biomarkers were also observed in the present cohort. Importantly, when the cohort was classified by Aβ- or tau-pathology, age-related elevated YKL-40 levels were more pronounced in individuals without AD pathology, whereas HGF, MIF, and TSP2 levels tended to be elevated in the presence of AD pathology. These differences are perhaps best ascribed to other pathology, such as amyotrophic lateral sclerosis (ALS) and Creutzfeldt-Jakob disease (CJD) (*31*), and modified production of YKL-40 is likely not related to AD. More important, changes in HGF, MIF and TSP2 at specific stages of Aβ and tau pathology indicate that they can serve as biological indicators of AD stage. In addition, the present findings support the notion that AD pathology is involved in regulating levels of HGF and MIF (*32, 33*). Thus, YKL-40 more likely reflects normal aging, whereas HGF, MIF, and TSP2 tend to be tightly linked to AD-pathology-driven glial cell senescence.

We observed that HGF, TSP2, LCN2, and serpinA3 levels were significantly modified only in Aβ+ individuals within the CDR>0 group and that there were similar concentrations in individuals with or without cognitive impairment. This suggests that these biomarkers may not be related to early cognitive impairment, but their expression is likely to be accelerated by Aβ once brain pathology reaches a certain stage. However, levels of YKL-40, which is closely related to neuronal injury (*34*), were positively correlated with cognitive decline in patients with or without AD pathology. Importantly, MIF levels also positively associated with CDR score, but only elevated in MCI and AD groups, which is in line with previous studies (*32*), indicating that MIF-mediated cognitive impairment was specifically related to AD pathology.

Thrombospondins, especially TSP1 and TSP2, are two major inhibitors of angiogenesis, which function on endothelial cell migration and the activity of vascular endothelial growth factor (VEGF) (*35*). An increase in angiogenesis is associated with neurological disorders (*36, 37*), such as PD dementia and stroke. Consistently, our data shows that TSP2 levels were lower in non-AD individuals. In contrast, TSP2 was elevated in Aβ- and tau- positive individuals with cognitive impairment. It has been suggested that

TSP2 is closely related to synaptogenesis and that astrocyte-secreted TSP2 is necessary for the formation of synapses (*25*). Thus, we should carefully consider the role of AD-pathology-driven expression of these senescent factors in the pathogenesis of AD.

SerpinA3 belongs to the serine protease inhibitor family and is involved in the pathogenesis of inflammation (*38*). We found that serpinA3 was abundant both in AD and non-AD human cortex, which is consistent with previous studies (*39, 40*) and with the fact that serpinA3 expression is upregulated in senescent glial cells (*15, 16*). Interestingly, CSF serpinA3 levels in AD individuals were comparable to those in the CN group and lower than that in non-AD group. SerpinA3 is reported to co-localize with Aβ (*26, 41, 42*), and we found that CSF serpinA3 levels were negatively correlated with the ratio of Aβ42/Aβ40, strongly suggesting that serpinA3 binds to Aβ plaque and that this may lead to the deposition of serpinA3 in brain and reduce secretion into CSF.

The diagnostic criteria of AD was updated in 2018 (*43*), which includes CSF and imaging markers of Aβ- and tau-pathology. Nevertheless, mixed forms of dementia may still result in an incorrect AD diagnosis of AD (*44*). Thus, it is necessary to discover new biomarkers to improve diagnostic accuracy. We found that levels of serpinA3 in CSF were specifically associated with Aβ pathology, and levels of TSP2 in CSF were markedly lower in non-AD individuals. Consistently, the LR model composed of serpinA3 and TSP2 improved the accuracy of AD diagnosis in our cohort, implying the possibility that aging-related biomarkers expressed by senescent glial cells can help distinguish AD from non-AD.

Our study has several limitations. First, it only recruited individuals from a single center, and multi-center cohorts are needed to confirm these results. Second, to determine the association of Aβ and tau pathology with CSF biomarkers, we defined our own cutoff values for Aβ42/Aβ40 and P-tau, which represent Aβ- and tau pathology, respectively. Thus, the suitability of these cutoff values needs to be verified before used for general clinical diagnosis. Third, it is a cross-sectional analysis, and longitudinal analysis should be combined to verify that biomarkers do change with aging.

In conclusion, our study shows that YKL40, HGF, MIF, and TSP2 are potential CSF biomarkers of senescent glial cells, providing novel insights into exploring aging in the living brain and monitoring clinical trials targeting senescent glial cells. Besides, we also identified some biomarkers, YKL-40, TSP2, or serpinA3, which are beneficial for discriminative accuracy in distinguishing MCI, AD, or non-AD patients from CN or AD patients from non-AD patients.

Acknowledgments

This work was supported by the National Key Plan for Scientific Research and Development of China (2020YFA0509304), the Chinese Academy of Sciences (QYZDY-SSW-SMC012 and XDB39000000), the National Natural Sciences Foundation of China (31530089), and the Fundamental Research Funds for the Central Universities (YD2070002003). HZ is a Wallenberg Scholar supported by grants from the Swedish Research Council (#2018-02532), the European Research Council (#681712), Swedish State Support for Clinical Research (#ALFGBG-720931), the Alzheimer Drug Discovery Foundation (ADDF), USA (#201809-2016862), the AD Strategic Fund and the Alzheimer's Association (#ADSF-21-831376-C, #ADSF-21-831381-C and #ADSF-21-831377-C), the Olav Thon Foundation, the Erling-Persson Family Foundation, Stiftelsen för Gamla Tjänarinnor, Hjärnfonden, Sweden (#FO2019-0228), the European Union’s Horizon 2020 research and innovation programme under the Marie Skłodowska-Curie grant agreement No 860197 (MIRIADE), and the UK Dementia Research Institute at UCL.

Author contribution

Y. S., F. G., and L. D. designed and initiated the study; X. L., Z. C., Y. W., Q. W., X. C., Q. T., and J. S. recruited patients and collected samples; F. G. and L. D. performed the experiments and analyzed the data; Y. S., F. G., and L. D. interpreted the data and wrote the manuscript.

Competing interests

HZ has served at scientific advisory boards and/or as a consultant for Abbvie, Alector, Eisai, Denali, Roche Diagnostics, Wave, Samumed, Siemens Healthineers, Pinteon Therapeutics, Nervgen, AZTherapies, CogRx, and Red Abbey Labs, has given lectures in symposia sponsored by Cellectricon, Fujirebio, Alzecure and Biogen, and is a co-founder of Brain Biomarker Solutions in Gothenburg AB (BBS), which is a part of the GU Ventures Incubator Program. The other authors declare that they have no competing financial interests.

Data availability

The data that support the findings of this study are available from the corresponding authors upon reasonable request.

References

1. P. Scheltens, B. De Strooper, M. Kivipelto, H. Holstege, G. Chetelat, C. E. Teunissen, J. Cummings, W. M. van der Flier, Alzheimer's disease. *Lancet*, (2021).
2. R. Di Micco, V. Krizhanovsky, D. Baker, F. d'Adda di Fagagna, Cellular senescence in ageing: from mechanisms to therapeutic opportunities. *Nature reviews. Molecular cell biology* **22**, 75-95 (2021).
3. D. J. Baker, K. B. Jeganathan, J. D. Cameron, M. Thompson, S. Juneja, A. Kopecka, R. Kumar, R. B. Jenkins, P. C. de Groen, P. Roche, J. M. van Deursen, BubR1 insufficiency causes early onset of aging-associated phenotypes and infertility in mice. *Nature genetics* **36**, 744-749 (2004).
4. V. Gorgoulis, P. D. Adams, A. Alimonti, D. C. Bennett, O. Bischof, C. Bishop, J. Campisi, M. Collado, K. Evangelou, G. Ferbeyre, J. Gil, E. Hara, V. Krizhanovsky, D. Jurk, A. B. Maier, M. Narita, L. Niedernhofer, J. F. Passos, P. D. Robbins, C. A. Schmitt, J. Sedivy, K. Vougas, T. von Zglinicki, D. Zhou, M. Serrano, M. Demaria, Cellular Senescence: Defining a Path Forward. *Cell* **179**, 813-827 (2019).
5. U. Gartner, M. Holzer, R. Heumann, T. Arendt, Induction of p21ras in Alzheimer pathology. *Neuroreport* **6**, 1441-1444 (1995).
6. A. McShea, P. L. Harris, K. R. Webster, A. F. Wahl, M. A. Smith, Abnormal expression of the cell cycle regulators P16 and CDK4 in Alzheimer's disease. *The American journal of pathology* **150**, 1933-1939 (1997).

7. T. Arendt, L. Rodel, U. Gartner, M. Holzer, Expression of the cyclin-dependent kinase inhibitor p16 in Alzheimer's disease. *Neuroreport* **7**, 3047-3049 (1996).
8. R. Bhat, E. P. Crowe, A. Bitto, M. Moh, C. D. Katsetos, F. U. Garcia, F. B. Johnson, J. Q. Trojanowski, C. Sell, C. Torres, Astrocyte senescence as a component of Alzheimer's disease. *PloS one* **7**, e45069 (2012).
9. R. Tiribuzi, A. Orlacchio, L. Crispoltoni, M. Maiotti, M. Zampolini, M. De Angeliz, P. Mecocci, R. Cecchetti, G. Bernardi, A. Datti, S. Martino, A. Orlacchio, Lysosomal beta-galactosidase and beta-hexosaminidase activities correlate with clinical stages of dementia associated with Alzheimer's disease and type 2 diabetes mellitus. *Journal of Alzheimer's disease : JAD* **24**, 785-797 (2011).
10. T. J. Bussian, A. Aziz, C. F. Meyer, B. L. Swenson, J. M. van Deursen, D. J. Baker, Clearance of senescent glial cells prevents tau-dependent pathology and cognitive decline. *Nature* **562**, 578-582 (2018).
11. P. Zhang, Y. Kishimoto, I. Grammatikakis, K. Gottimukkala, R. G. Cutler, S. Zhang, K. Abdelmohsen, V. A. Bohr, J. Misra Sen, M. Gorospe, M. P. Mattson, Senolytic therapy alleviates Abeta-associated oligodendrocyte progenitor cell senescence and cognitive deficits in an Alzheimer's disease model. *Nature neuroscience* **22**, 719-728 (2019).
12. S. Jakel, L. Dimou, Glial Cells and Their Function in the Adult Brain: A Journey through the History of Their Ablation. *Frontiers in cellular neuroscience* **11**, 24 (2017).
13. A. D. Greenhalgh, S. David, F. C. Bennett, Immune cell regulation of glia during CNS injury and disease. *Nature reviews. Neuroscience* **21**, 139-152 (2020).
14. L. Soreq, U. K. B. E. Consortium, C. North American Brain Expression, J. Rose, E. Soreq, J. Hardy, D. Trabzuni, M. R. Cookson, C. Smith, M. Ryten, R. Patani, J. Ule, Major Shifts in Glial Regional Identity Are a Transcriptional Hallmark of Human Brain Aging. *Cell reports* **18**, 557-570 (2017).
15. L. E. Clarke, S. A. Liddelow, C. Chakraborty, A. E. Munch, M. Heiman, B. A. Barres, Normal aging induces A1-like astrocyte reactivity. *Proceedings of the National Academy of Sciences of the United States of America* **115**, E1896-E1905 (2018).
16. M. M. Boisvert, G. A. Erikson, M. N. Shokhirev, N. J. Allen, The Aging Astrocyte Transcriptome from Multiple Regions of the Mouse Brain. *Cell reports* **22**, 269-285 (2018).
17. W. T. Wong, Microglial aging in the healthy CNS: phenotypes, drivers, and rejuvenation. *Frontiers in cellular neuroscience* **7**, 22 (2013).
18. D. L. Gruol, Impact of Increased Astrocyte Expression of IL-6, CCL2 or CXCL10 in Transgenic Mice on Hippocampal Synaptic Function. *Brain sciences* **6**, (2016).
19. M. Verkerke, E. M. Hol, J. Middeldorp, Physiological and Pathological Ageing of Astrocytes in the Human Brain. *Neurochemical research*, (2021).
20. B. V. Lananna, C. A. McKee, M. W. King, J. L. Del-Aguila, J. M. Dimitry, F. H. G. Farias, C. J. Nadarajah, D. D. Xiong, C. Guo, A. J. Cammack, J. A. Elias, J.

Zhang, C. Cruchaga, E. S. Musiek, Chi3l1/YKL-40 is controlled by the astrocyte circadian clock and regulates neuroinflammation and Alzheimer's disease pathogenesis. *Science translational medicine* **12**, (2020).

21. R. Craig-Schapiro, R. J. Perrin, C. M. Roe, C. Xiong, D. Carter, N. J. Cairns, M. A. Mintun, E. R. Peskind, G. Li, D. R. Galasko, C. M. Clark, J. F. Quinn, G. D'Angelo, J. P. Malone, R. R. Townsend, J. C. Morris, A. M. Fagan, D. M. Holtzman, YKL-40: a novel prognostic fluid biomarker for preclinical Alzheimer's disease. *Biological psychiatry* **68**, 903-912 (2010).
22. T. M. Greco, S. H. Seeholzer, A. Mak, L. Spruce, H. Ischiropoulos, Quantitative mass spectrometry-based proteomics reveals the dynamic range of primary mouse astrocyte protein secretion. *Journal of proteome research* **9**, 2764-2774 (2010).
23. S. Lee, J. Y. Park, W. H. Lee, H. Kim, H. C. Park, K. Mori, K. Suk, Lipocalin-2 is an autocrine mediator of reactive astrocytosis. *The Journal of neuroscience : the official journal of the Society for Neuroscience* **29**, 234-249 (2009).
24. F. Brozzi, C. Arcuri, I. Giambanco, R. Donato, S100B Protein Regulates Astrocyte Shape and Migration via Interaction with Src Kinase: IMPLICATIONS FOR ASTROCYTE DEVELOPMENT, ACTIVATION, AND TUMOR GROWTH. *The Journal of biological chemistry* **284**, 8797-8811 (2009).
25. K. S. Christopherson, E. M. Ullian, C. C. Stokes, C. E. Mullowney, J. W. Hell, A. Agah, J. Lawler, D. F. Mosher, P. Bornstein, B. A. Barres, Thrombospondins are astrocyte-secreted proteins that promote CNS synaptogenesis. *Cell* **120**, 421-433 (2005).
26. C. R. Abraham, Reactive astrocytes and alpha1-antichymotrypsin in Alzheimer's disease. *Neurobiology of aging* **22**, 931-936 (2001).
27. G. M. McKhann, D. S. Knopman, H. Chertkow, B. T. Hyman, C. R. Jack, Jr., C. H. Kawas, W. E. Klunk, W. J. Koroshetz, J. J. Manly, R. Mayeux, R. C. Mohs, J. C. Morris, M. N. Rossor, P. Scheltens, M. C. Carrillo, B. Thies, S. Weintraub, C. H. Phelps, The diagnosis of dementia due to Alzheimer's disease: recommendations from the National Institute on Aging-Alzheimer's Association workgroups on diagnostic guidelines for Alzheimer's disease. *Alzheimer's & dementia : the journal of the Alzheimer's Association* **7**, 263-269 (2011).
28. B. Winblad, K. Palmer, M. Kivipelto, V. Jelic, L. Fratiglioni, L. O. Wahlund, A. Nordberg, L. Backman, M. Albert, O. Almkvist, H. Arai, H. Basun, K. Blennow, M. de Leon, C. DeCarli, T. Erkinjuntti, E. Giacobini, C. Graff, J. Hardy, C. Jack, A. Jorm, K. Ritchie, C. van Duijn, P. Visser, R. C. Petersen, Mild cognitive impairment--beyond controversies, towards a consensus: report of the International Working Group on Mild Cognitive Impairment. *Journal of internal medicine* **256**, 240-246 (2004).
29. C. R. Jack, Jr., D. A. Bennett, K. Blennow, M. C. Carrillo, H. H. Feldman, G. B. Frisoni, H. Hampel, W. J. Jagust, K. A. Johnson, D. S. Knopman, R. C. Petersen, P. Scheltens, R. A. Sperling, B. Dubois, A/T/N: An unbiased descriptive classification scheme for Alzheimer disease biomarkers. *Neurology* **87**, 539-547

(2016).
30. H. Mathys, J. Davila-Velderrain, Z. Peng, F. Gao, S. Mohammadi, J. Z. Young, M. Menon, L. He, F. Abdurrob, X. Jiang, A. J. Martorell, R. M. Ransohoff, B. P. Hafler, D. A. Bennett, M. Kellis, L. H. Tsai, Single-cell transcriptomic analysis of Alzheimer's disease. *Nature* **570**, 332-337 (2019).
31. P. Andres-Benito, R. Dominguez, M. J. Colomina, F. Llorens, M. Povedano, I. Ferrer, YKL40 in sporadic amyotrophic lateral sclerosis: cerebrospinal fluid levels as a prognosis marker of disease progression. *Aging* **10**, 2367-2382 (2018).
32. A. Oikonomidi, D. Tautvydaite, M. M. Gholamrezaee, H. Henry, M. Bacher, J. Popp, Macrophage Migration Inhibitory Factor is Associated with Biomarkers of Alzheimer's Disease Pathology and Predicts Cognitive Decline in Mild Cognitive Impairment and Mild Dementia. *Journal of Alzheimer's disease : JAD* **60**, 273-281 (2017).
33. Y. Tsuboi, K. Kakimoto, M. Nakajima, H. Akatsu, T. Yamamoto, K. Ogawa, T. Ohnishi, Y. Daikuhara, T. Yamada, Increased hepatocyte growth factor level in cerebrospinal fluid in Alzheimer's disease. *Acta neurologica Scandinavica* **107**, 81-86 (2003).
34. F. Baldacci, S. Lista, E. Cavedo, U. Bonuccelli, H. Hampel, Diagnostic function of the neuroinflammatory biomarker YKL-40 in Alzheimer's disease and other neurodegenerative diseases. *Expert review of proteomics* **14**, 285-299 (2017).
35. P. R. Lawler, J. Lawler, Molecular basis for the regulation of angiogenesis by thrombospondin-1 and -2. *Cold Spring Harbor perspectives in medicine* **2**, a006627 (2012).
36. S. Janelidze, D. Lindqvist, V. Francardo, S. Hall, H. Zetterberg, K. Blennow, C. H. Adler, T. G. Beach, G. E. Serrano, D. van Westen, E. Londos, M. A. Cenci, O. Hansson, Increased CSF biomarkers of angiogenesis in Parkinson disease. *Neurology* **85**, 1834-1842 (2015).
37. G. Zadeh, A. Guha, Angiogenesis in nervous system disorders. *Neurosurgery* **53**, 1362-1374; discussion 1374-1366 (2003).
38. S. T. Chelbi, M. L. Wilson, A. C. Veillard, S. A. Ingles, J. Zhang, F. Mondon, G. Gascoin-Lachambre, L. Doridot, T. M. Mignot, R. Rebourcet, B. Carbonne, J. P. Concordet, S. Barbaux, D. Vaiman, Genetic and epigenetic mechanisms collaborate to control SERPINA3 expression and its association with placental diseases. *Human molecular genetics* **21**, 1968-1978 (2012).
39. J. Padmanabhan, M. Levy, D. W. Dickson, H. Potter, Alpha1-antichymotrypsin, an inflammatory protein overexpressed in Alzheimer's disease brain, induces tau phosphorylation in neurons. *Brain : a journal of neurology* **129**, 3020-3034 (2006).
40. C. Chen, X. F. Xu, R. Q. Zhang, Y. Ma, Y. Lv, J. L. Li, Q. Shi, K. Xiao, J. Sun, X. D. Yang, Q. Shi, X. P. Dong, Remarkable increases of alpha1-antichymotrypsin in brain tissues of rodents during prion infection. *Prion* **11**, 338-351 (2017).
41. P. E. Fraser, J. T. Nguyen, D. R. McLachlan, C. R. Abraham, D. A. Kirschner,

Alpha 1-antichymotrypsin binding to Alzheimer A beta peptides is sequence specific and induces fibril disaggregation in vitro. *Journal of neurochemistry* **61**, 298-305 (1993).

42. F. Licastro, S. Pedrini, L. Caputo, G. Annoni, L. J. Davis, C. Ferri, V. Casadei, L. M. Grimaldi, Increased plasma levels of interleukin-1, interleukin-6 and alpha-1-antichymotrypsin in patients with Alzheimer's disease: peripheral inflammation or signals from the brain? *Journal of neuroimmunology* **103**, 97-102 (2000).
43. C. R. Jack, Jr., D. A. Bennett, K. Blennow, M. C. Carrillo, B. Dunn, S. B. Haeberlein, D. M. Holtzman, W. Jagust, F. Jessen, J. Karlawish, E. Liu, J. L. Molinuevo, T. Montine, C. Phelps, K. P. Rankin, C. C. Rowe, P. Scheltens, E. Siemers, H. M. Snyder, R. Sperling, Contributors, NIA-AA Research Framework: Toward a biological definition of Alzheimer's disease. *Alzheimer's & dementia : the journal of the Alzheimer's Association* **14**, 535-562 (2018).
44. K. M. Langa, N. L. Foster, E. B. Larson, Mixed dementia: emerging concepts and therapeutic implications. *Jama* **292**, 2901-2908 (2004).

Figure and Tables

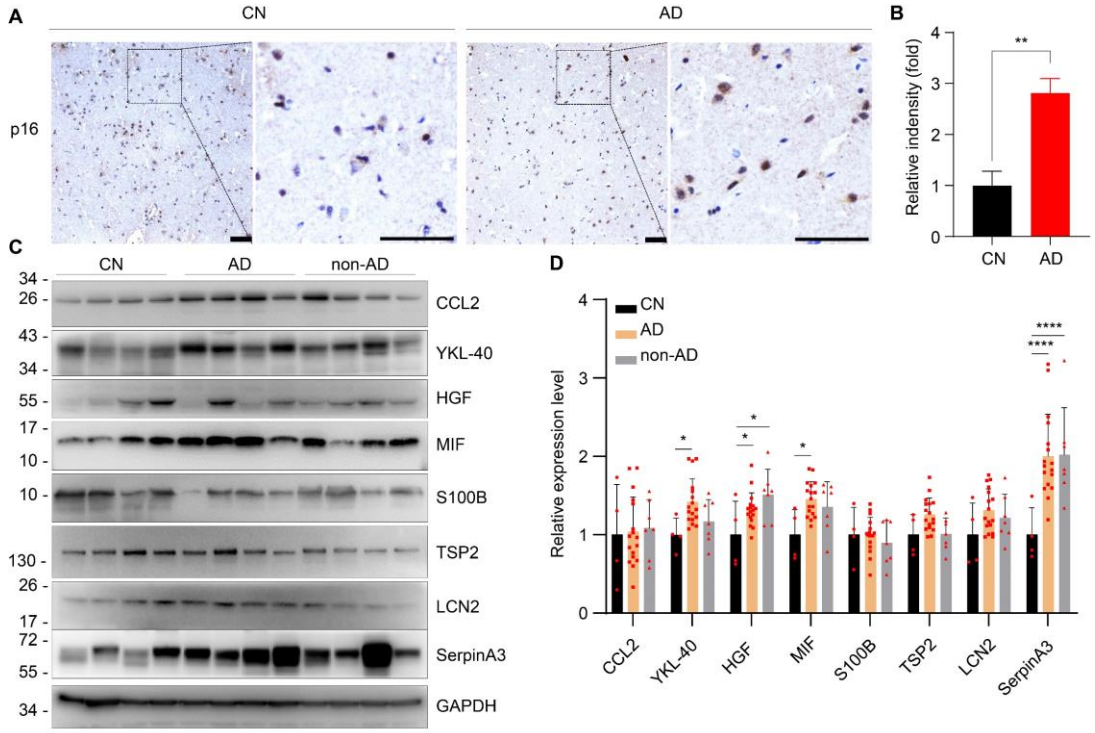

Fig.1 Accumulation of senescent cells in the AD brain. (A) p16 immunohistochemical staining of the frontal cortex of AD patients and age-matched controls. Scale bar=50 μm. **(B)** Quantification of p16-positive dots (*n*=5 CN and 9 AD participants; 5 images were analyzed in sections from each participant). Data are mean ± s.e.m. $^{**}P < 0.01$ (two-sided Student's t-test) **(C)** Immunoblot analysis of aging-related molecules in the frontal cortex of CN, AD, and non-AD individuals. **(D)** Quantification of the immunoreactive bands as those shown in (C). Data are means ± s.e.m. $^{*}P < 0.05$; $^{****}P < 0.0001$ (two-way ANOVA followed by Bonferroni correction)

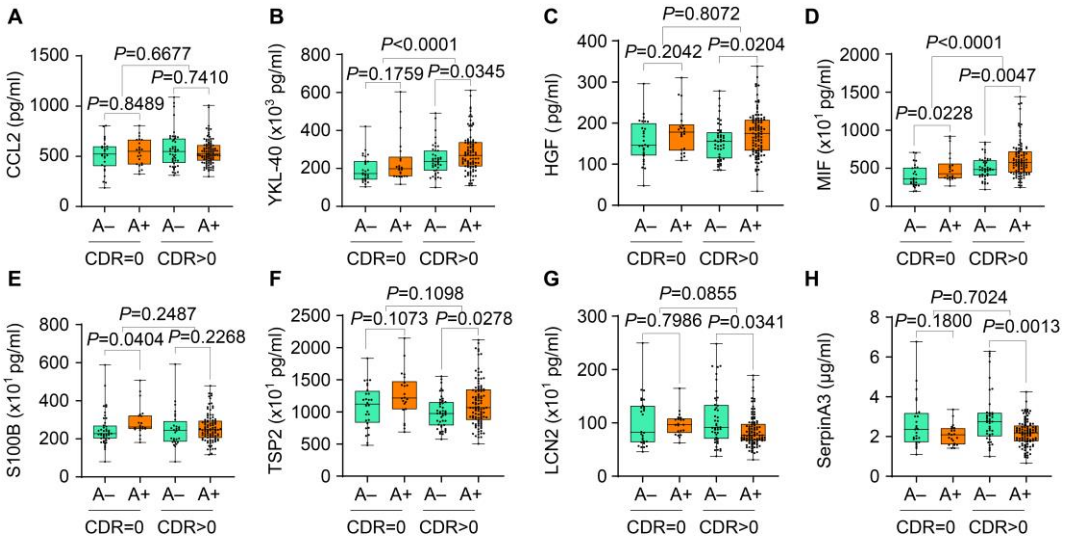

Fig.2 Comparison of CSF biomarkers levels with Aβ status and CDR score. Dot and box plots depicting levels of CSF biomarkers across all groups and separated by Aβ status and CDR score. The box plots depict the median (horizontal bar), interquartile range (IQR, hinges), and the whiskers indicate the minimum and maximum values. *P*-values were assessed by a one-way analysis of covariance (ANCOVA) adjusted by age, gender, and *APOE*-ε4. **P*<0.05; ***P*<0.01; ****P*<0.001; *****P*<0.0001.

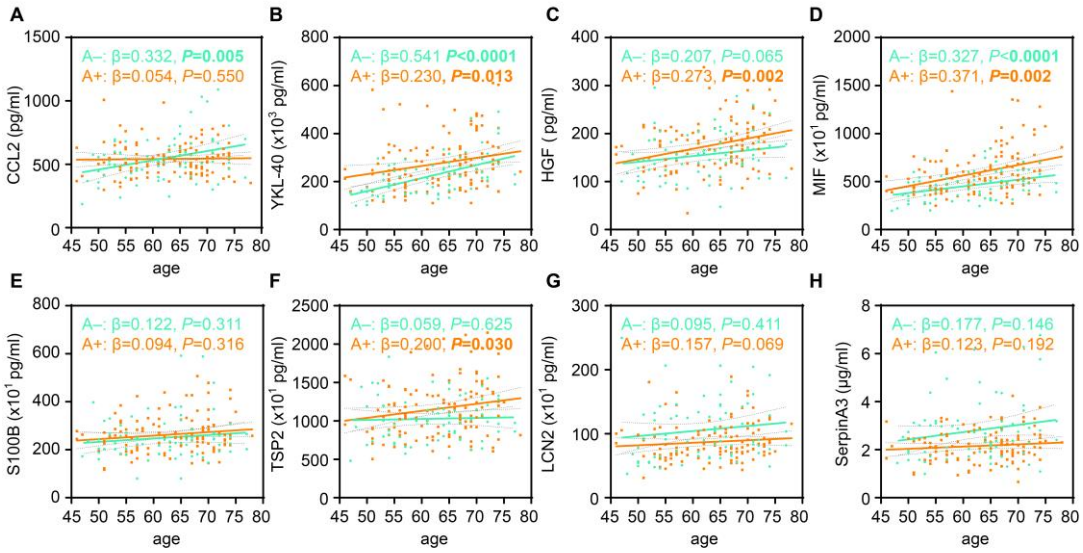

Fig.3 Association of CSF biomarkers with age. Scatter plots representing the correlation of each of the demographic characteristics with age in the A– and the A+ groups. Each point depicts the value of the CSF biomarker of an individual and the solid lines indicate the regression line for each group. The standardized regression coefficients (β) and the *P*-values are shown and were computed using a linear model adjusting for age, gender, and *APOE*-ε4.

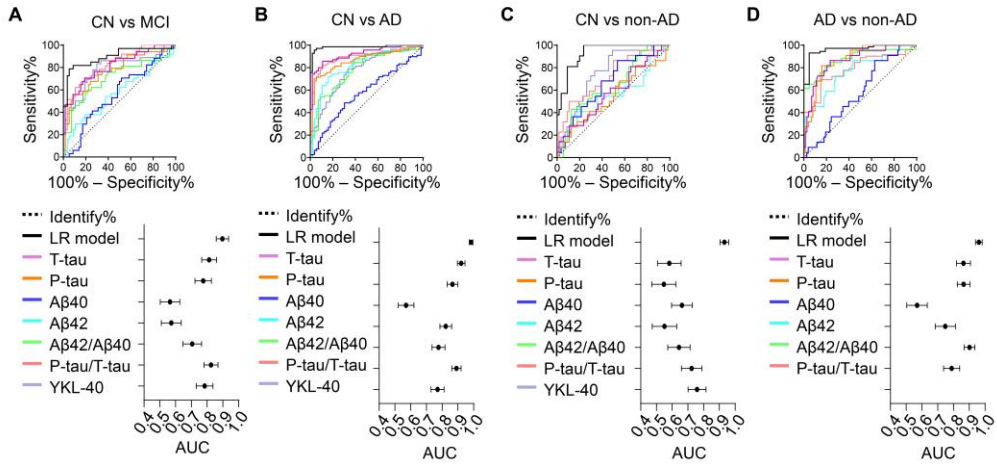

Fig.4 Receiver operating characteristic (ROC) curves for classification of different diagnostic groups. The LR model includes the following variables: **(A)** T-tau, Aβ40, YKL-40, and *APOE* state. **(B)** T-tau, Aβ40, Aβ42, YKL-40 and *APOE* state. **(C)** T-tau, Aβ40, Aβ42, Aβ42/ Aβ40 and YKL-40. **(D)** T-tau, Aβ42, TSP2, serpinA3 and *APOE* state. (*APOE* state : 0 for no *APOE*-ε4 carriers, 1 for *APOE*-ε4 carriers)

Table 1. Clinical details of human brain tissue

Subjects	Pathology	PMD (h)	Gender	Age (yrs)	Use
Control 1	Normal	48	F	96	IHC/WB
Control 2	Normal	17	M	59	IHC/WB
Control 3	Normal	20	M	66	IHC/WB
Control 4	Normal	17	M	73	IHC/WB
Control 5	Normal	4	F	75	IHC
non-AD 1	DLB	22	F	69	WB
non-AD 2	DLB	13	F	77	WB
non-AD 3	DLB	9	M	83	WB
non-AD 4	DLB	9	M	63	WB
non-AD 5	FTD	5	M	51	WB
non-AD 6	Pick's disease	5.5	M	81	WB
non-AD 7	DLB/PD	4	M	79	WB
AD 1	AD	5	F	81	IHC/WB
AD 2	AD	5	F	93	IHC/WB
AD 3	AD	6	F	97	IHC/WB
AD 4	AD	4	M	73	IHC/WB
AD 5	AD	5	M	83	IHC/WB
AD 6	AD	4	F	80	IHC/WB
AD 7	AD	4	M	81	IHC/WB
AD 8	AD	3	M	81	IHC/WB
AD 9	AD	5	M	79	IHC/WB

AD 10	AD	4	F	82	WB
AD 11	AD	5	M	67	WB
AD 12	AD	4	F	71	WB
AD 13	AD	4	F	80	WB
AD 14	AD	5	F	80	WB
AD 15	AD	4	M	75	WB
AD 16	AD	9	F	70	WB
AD 17	AD	4	F	83	WB

DLB, dementia with Lewy bodies; FTD, frontotemporal dementia; PD, Parkinson's Disease; AD, Alzheimer’s disease; non-AD, non-Alzheimer’s disease dementia; IHC, immunohischemistry; WB: Western blotting; PMD, postmortem delay; yrs, years.

Table 2. Demographic characteristics of subjects

		Total (n=195)	CN (n=58, 29.7%)	MCI (n=37, 19.0%)	AD (n=78, 40.0%)	non-AD (n=22, 11.3%)
Gender, M/F		83/112 (42.6%)	29/29 (50.0%)	16/21 (43.2%)	28/50 (56.0%)	10/12 (45.5%)
Age, years						
	Mean±SD	62.83±7.71	60.28±8.35[b,c]	66±6.56[a]	63.76±7.25[a]	60.95±7.17
	Median	64.0	61.0	68.0	65.0	61.5
	95% CI	61.74, 63.92	58.08, 62.47	63.98, 68.41	62.09, 65.43	57.78, 64.13
Education, years						
	Mean±SD	7.23±4.61	7.03±4.48	8.35±4.88	6.88±4.57	7.05±4.63
	Median	8.0	7.0	9.0	7.5	8.0
	95% CI	6.57, 7.88	5.86, 8.21	6.59, 9.91	5.81, 7.96	4.99, 9.10
MMSE						
	Mean±SD	18.88±8.22	27.05±3.39[b,c,d]	21.11±4.52[a,c,d]	12.83±6.48[a,b]	14.5±7.52[a,b]
	Median	20.0	28.0	21.0	13.0	14.5
	95% CI	17.71, 20.05	26.16, 27.94	19.42, 22.42	11.29, 14.29	11.17, 17.83
CDR						
	Mean±SD	0.82±0.72	0.12±0.31[b,c,d]	0.51±0.22[a,c,d]	1.43±0.57[a,b,d]	1.14±0.52[a,b,c]
	Median	1.0	0	0.5	1	1
	95% CI	0.72, 0.93	0.04, 0.20	0.44, 0.59	1.30, 1.56	0.91, 1.37
***APOE-ε4* carriers, n (%)**		76 (39.0%)	7 (12.1%)[b,c]	19 (51.4)[a,d]	47 (60.3%)[a,d]	3 (13.6%) [b,c]

[a]Significant values vs CN; [b]Significant values vs MCI; [c]Significant values vs AD; [d]Significant values vs non-AD.

Table 3. CSF molecules concentrations and ratios of subjects

	Total (n=195)	CN (n=58, 29.7%)	MCI (n=37, 19.0%)	AD (n=78, 40.0%)	non-AD (n=22, 11.3%)
T-tau（pg/ml）	361.94±263.21	194.03±79.38[b,c]	367.94±216.78[a,c]	532.2±301.44[a,b,d]	229.82±127.46[c]

P- tau（pg/ml）	61.32±27.24	45.11±14.12[b,c]	64.82±22.24[a,c,d]	77.66±29.31[a,b,d]	42.44±16.06[b,c]
Aβ40（pg/ml）	7858±3928.46	8424.79±4304.42	9083.46±3494.48[d]	7405.16±3961.54	6019.7±2408.87[b]
Aβ42（pg/ml）	388.66±189.42	467.18±191.29[c]	444.18±232.53[c]	289.39±102.47[a,b,d]	447.37±197.31[c]
Aβ42/Aβ40	0.0543±0.021	0.0628±0.0178[b,c]	0.0497±0.0231[a,d]	0.0453±0.0184[a,d]	0.0721±0.0134[b,c]
P-tau/T-tau	0.1961±0.0588	0.2432±0.0448[b,c,d]	0.19±0.0391[a,c]	0.1625±0.0528[a,b,d]	0.2015±0.0572[a,c]
CCL2（pg/ml）	543.57±146.14	523.3±155.53	565.5±154.07	547.51±123.36	546.3±181.15
YKL-40（pg/ml）	256797.8±103248.6	195813.5±63605.9[b,c,d]	298492.3±115083.7[a]	281570.3±107155.8[a]	262123.7±85570.3[a]
HGF（pg/ml）	168.1±52.18	160.9±45.73	183.86±56.31[d]	171.09±56.09	150±39.38[b]
MIF（pg/ml）	5497.78±2163.48	4238.23±1522.43[b,c]	5587.16±1497.66[a]	6427.32±2524.57[a]	5306.49±1387.38
S100B（pg/ml）	2603.74±865.44	2614.5±856.08	2797.2±919.15	2604.58±807.34	2256.31±951.08
TSP2（pg/ml）	11119.86±3397.73	11116±3713.96	11955.9±2833.31[d]	11320.67±3499.54[d]	9012.02±2123.19[b,c]
LCN2（pg/ml）	940.09±385.04	939.53±385.64	933.98±341.96	905.32±386.42	1081.56±442.29
SerpinA3（μg/ml）	2.39±0.98	2.4±0.98[d]	2.24±0.84[d]	2.25±0.80[d]	3.15±1.42[a,b,c]

[a]Significant values vs CN; [b]Significant values vs MCI; [c]Significant values vs AD; [d]Significant values vs non-AD

Table 4. Association between CSF molecules and AD hallmarks

		CCL2	YKL-40	HGF	MIF	S100B	TSP2	LCN2	SerpinA3
T-tau	Unstandardized B (SE)	-0.02 (0.04)	119.54 (27.04)	0.05 (0.01)	4.03 (0.43)	0.22 (0.26)	3.03 (0.95)	-0.13 (0.11)	0 (0)
	Standardized β	-0.03	0.31	0.27	0.53	0.07	0.24	-0.09	-0.13

	P value	0.684	**<0.001**	**<0.001**	**<0.001**	0.393	**0.002**	0.219	0.089
P-tau	Unstandardized B (SE)	-0.29 (0.4)	1136.61 (263.11)	0.63 (0.13)	43.89 (3.86)	4.80 (2.44)	41.82 (8.89)	-2.35 (1.02)	-0.01 (0)
	Standardized β	-0.05	0.3	0.33	0.6	0.15	0.34	-0.17	-0.16
	P value	0.478	**<0.001**	**<0.001**	**<0.001**	0.051	**<0.001**	**0.022**	**0.037**
Aβ40	Unstandardized B (SE)	0(0)	2.41 (1.85)	0 (0)	0.21 (0.03)	0.03 (0.02)	0.33 (0.06)	-0.02 (0.01)	0 (0)
	Standardized β	0.02	0.09	0.38	0.37	0.12	0.39	-0.2	-0.18
	P value	0.751	0.196	**<0.001**	**<0.001**	0.107	**<0.001**	**0.004**	**0.02**
Aβ42	Unstandardized B (SE)	0.13 (0.06)	-18.81 (39.36)	0.05 (0.02)	0.27 (0.78)	-0.08 (0.35)	3.75 (1.32)	0.05 (0.15)	0 (0)
	Standardized β	0.17	-0.03	0.19	0.02	-0.02	0.21	0.02	0.08
	P value	**0.025**	0.633	**0.007**	0.734	0.824	**0.005**	0.757	0.289
Aβ42/Aβ40	Unstandardized B (SE)	339.98 (516.86)	-1048019.32 (349891.67)	-638.86 (171.04)	-35142.91 (6612.18)	-7036.95 (3077.12)	-45600.71 (11710.93)	5715.15 (1234.06)	15.37 (3.35)
	Standardized β	0.05	-0.21	-0.26	-0.34	-0.17	-0.28	0.31	0.33
	P value	0.511	**0.003**	**<0.001**	**<0.001**	**0.023**	**<0.001**	**<0.001**	**<0.001**
P-Tau/T-tau	Unstandardized B (SE)	-286.08 (183.08)	-608473.24 (118056.41)	-138.56 (62.31)	-13038.24 (2327.56)	1341.64 (1103.49)	-4688.71 (4314.34)	-236.24 (472.85)	1.75 (1.28)
	Standardized β	-0.11	-0.35	-0.16	-0.36	0.09	-0.08	-0.04	0.10
	P value	0.12	**<0.001**	**0.027**	**<0.001**	0.226	0.279	0.618	0.172

Each biomarker as a dependent variable was assessed by a linear model with age, sex and *APOE-ε4* status as independent variables. The unstandardized regression coefficients (B), standard errors (SE), standardized regression coefficients (β) and *P*-values are shown.

Table 5. Association between CSF molecules and age

		CCL2	YKL-40	HGF	MIF	S100B	TSP2	LCN2	SerpinA3
age	Unstandardized B (SE)	3.09 (1.35)	4447.43 (919.38)	1.87 (0.47)	101.24 (18.86)	13.84 (8.03)	67.01 (31.35)	4.48 (3.59)	0.01 (0.01)
	Standardized β	0.16	0.33	0.28	0.36	0.12	0.15	0.09	0.11
	P value	**0.023**	**<0.001**	**<0.001**	**<0.001**	0.087	**0.034**	0.214	0.123

Each biomarker as a dependent variable was assessed by a linear model with age as independent variables. The unstandardized regression coefficients (B), standard errors (SE), standardized regression coefficients (β) and P-values are shown.